Design and Analysis of a Robotic Arm for a Commercial Flight Simulator

Haifa El-Sadi
Mechanical Engineering
Wentworth Institute of Technology
Boston, USA
E-mail: elsadih@wit.edu

John Connolly
Mechanical Engineering
Wentworth Institute of Technology
Boston, USA
E-mail: connollyj@wit.edu

***Abstract*—This study is an elementary design and analysis of a novel flight simulator design. The simulator is positioned at the end of a large 5-axis robotic arm. The robot was designed in three configurations for different implementations, the principal application being a Boeing 747 simulator. The main purpose of this design is to give pilots an accurate experience with a wide range of motion up to 2g of acceleration.**

This paper describes the design objectives and the methodology to accomplish the goals. It includes preliminary designs and detailed CAD models. To validate the safety of the design, stress analysis was conducted under gravity loading and maximum dynamic loading.

Keywords-Simulator; CAD; Stress; Robot

I. INTRODUCTION

In the 1950s, companies began building virtual cockpits that simulated the experience of flight for pilots. Flight simulators would replicate each aspect of flying the actual aircraft for the pilots: controls, visuals, and motion. This tool allows for excellent, accurate training without any risk or cost of flying actual aircraft. Changes in the design of software algorithms for generating physical motion in flight simulators have typically been put forward on the grounds of improved motion cueing. Meyer et al. studied the pilot evaluations of algorithms implemented on a six degree of freedom flight simulator simulation a large transport aircraft during low altitude flight [1].

Previous studies attempted to quantify the perceptions of airline pilots about the quality of motion possible when a number of different motion-drive algorithms which were tested on a simulator employing a state-of-art six degrees of freedom motion-base [2]. Eric et al. described a new approach to relate simulator sickness ratings with the main frequency component of the simulator motion mismatch, that is, the computed difference between the time histories of simulator motion and vehicle motion [3]. The simulator motion cueing problem has been considered extensively, some studies showed that a cueing algorithm, that can make better use of the platform workspace whilst ensuring that its bounds are never exceeded [4].

There are simulators with a duplicate cockpit of the Boeing 777 on the top. A trainee sits inside, and screens give the pilot a virtual view of the world. The simulator sits a top six hydraulic legs. To simulate motion during flight, these hydraulic cylinders are finely controlled by electric pumps.

For example, extending the front legs would tilt the simulator backward. The pilots would experience being pulled into their seats. This type of motion could simulate linear acceleration of the aircraft. Conversely, if the back legs were raised and the front lowered, the pilots would be pulled forward. This would simulate braking. On the other hand, a hexapod system allows for six degrees of freedom: linear motion in all axes (x, y, z), as well as rotational motion (roll, pitch, yaw). However, the system is extremely limited in motion. This means simulated movements are short duration and mostly limited to 1G. For example, the acceleration a pilot may feel on the runway in the x-direction might typically be 0.3G. When added to the force of gravity, a pilot will feel a resultant force over a G. These simulators will only be able to produce 1G for the pilot. Although this hydraulic system retains a small footprint, a wider range of motion would allow for more accurately representation of motion.

The objective of this project is to accurately simulate the motion of a Boeing 747 using a robotic arm. The motion of a 747 can be described in five axes of motion: 2 translational, 3 rotational. Thus, a flight simulator built upon a robotic arm requires five degrees of freedom. The system must replicate the g-forces experienced by a pilot during flight of a 747. This paper will detail the design process for this system. After developing a motion profile, the virtual cockpit's weight will be used to develop the system's dynamic and broad electrical requirements. An iterative process of modeling and stress analysis will be used to design the arm. Finally, a motion analysis will validate the system provides the required motion.

II. ROBOT ARM CONFIGURATION

Each of the five degrees of motion (two linear, three rotational) must be simulated with the robot arm (as outlined above, IV. 747 Motion Profile). The robot's configuration is a tandem application of a traditional robot arm and a gyroscopic wrist. The pilot will only experience two translational accelerations at any given instant; therefore, the robot arm only needs to supply two degrees of translational motion. This significantly simplifies the configuration of the arm. The virtual cockpit (simulator box) will be mounted at the end effector of the robot arm. The end effector must be able to supply all three degrees of rotation (roll, pitch, yaw). Figure 1 shows the basic robot configurations. However, Figure 2 shows the shoulder and arm function (simulated translational motion), and Gyroscopic wrist function (rotational motion).

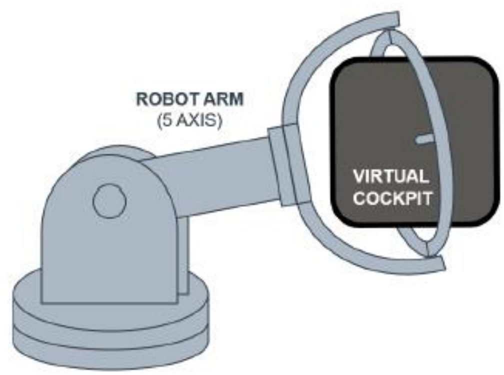

Figure 1. Basic robot configuration

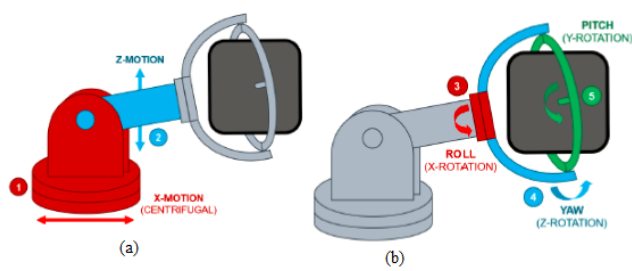

Figure 2. (a) Shoulder and arm function (simulated translational motion), (b) Gyroscopic wrist function (rotational motion)

An objective of the robot's design is to be capable of simulating the complete flight motion of the 747. A statistical study published by the Federal Flight Administration describes the loading conditions of the 747 through flight phases.

To create a maximum resultant load, each of the accelerations will be added as vectors and combined with the system's weights. Although flight may not ever experience 2g at any one instant, this allows for worst case conditions and inherits a factor of safety. Once each components weight is determined and a factor of safety is applied, the stress simulations can be applied with these loads. As shown in Figure 3, each part of the robot must be able to withstand 2g of acceleration. Using each components weight and a factor of safety of 1.5, the max loading conditions can be calculated. Figure 3 describes the image of each of the major robot components and the system's joints.

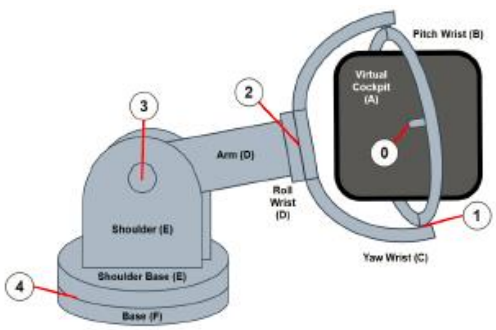

Figure 3. Robot Components (A-F) Robot Joints (0-4)

III. ROBOT MODELS

The simulator model is shown in Figure 4. The model is parametric such that characteristic of the design can easily be changed and updated throughout the model. Each component is designed such that the pin and joint is safe to meet the factor of safety requirement at max loading.

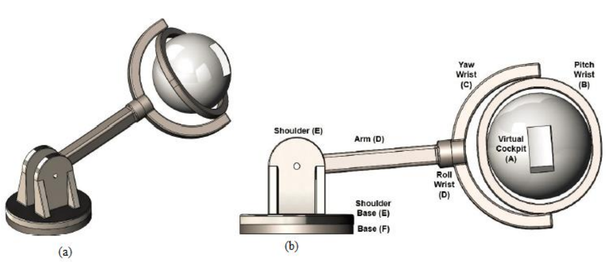

Figure 4. Simulator Isometric view (a) Labeled components (b)

The robot is structurally constructed of 1020 mild steel. This material was selected for its wide manufacturability. The large pins at each joint are machined from 316 stainless steel for its strength as shown in Figure 5.

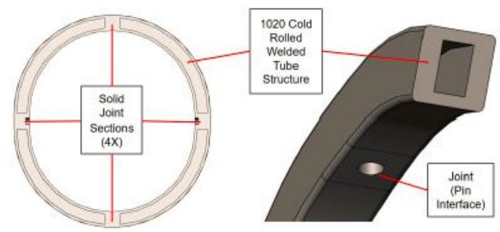

Figure 5. Pitch wrist cross section and structure

At the pin joints, a solid machined section interfaces with the pin. It is solid because of the stress concentrations at these points. The rest of the structure is created by welding four machined and fabricated plates together to create the tube shown in Figure 6. Shown below is the cross section of the robot which uses this general structure: solid joint sections and structural tubes. This allows for rigid joints at stress concentrations. The tubing structure keeps the weight low but maintains rigidity.

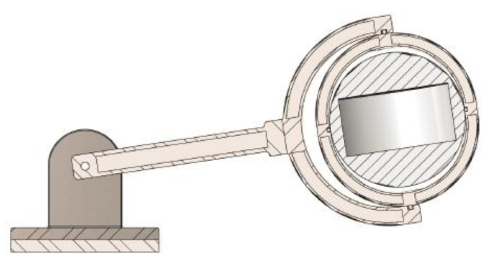

Figure 6. Robot Cross Section

Being a novel design, three configurations of the robot will be designed and simulated. Using a parametric model, each configuration is easily modeled and simulated. The configurations will represent possible implementations. In each version, the radius of the spherical virtual cockpit and the cockpit weight are the principle changes. This cascades to geometry and weight of the pitch and yaw wrist components. However, the tube's cross-sectional dimensions (wall thickness, width) remain constant. The shoulder and arm geometry remain the same through each version as shown in Figure 7.

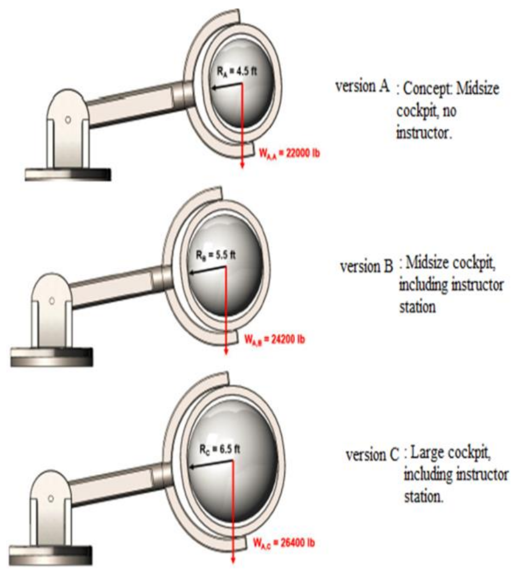

Figure 7. Different versions of cockpit

IV. STRESS ANALYSIS

Stress analysis was performed to ensure the safety of each of the robot component. Using SolidWorks static simulation, each component is simulated in its axis which is most susceptible to failure. Each component is designed to be safe for at least 2g of acceleration (and a FOS of 1.15). The static gravity load will also be simulated. Figure 8 shows, ach of the components are meshed using a blended curvature-based mesh. This meshing method is the best available in SolidWorks for the complex geometry of these models. Mesh controls are applied at stress concentration points to increase the accuracy of the simulation results at the failure points. For each component of each version, the meshes and conditions will be tabulated. In these plots, the purple and green arrows represent the loads and the fixtures, respectively. Additionally, the Von Mises stress plots will be tabulated for both the static gravity load and the dynamic 2g load.

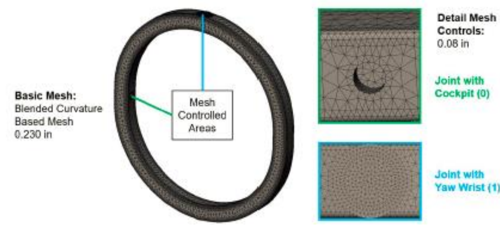

Figure 8. Mesh details for the pitch wrist component (version A)

Figures 9, 10 and 11 show the stress analysis of version A, version B and version C.

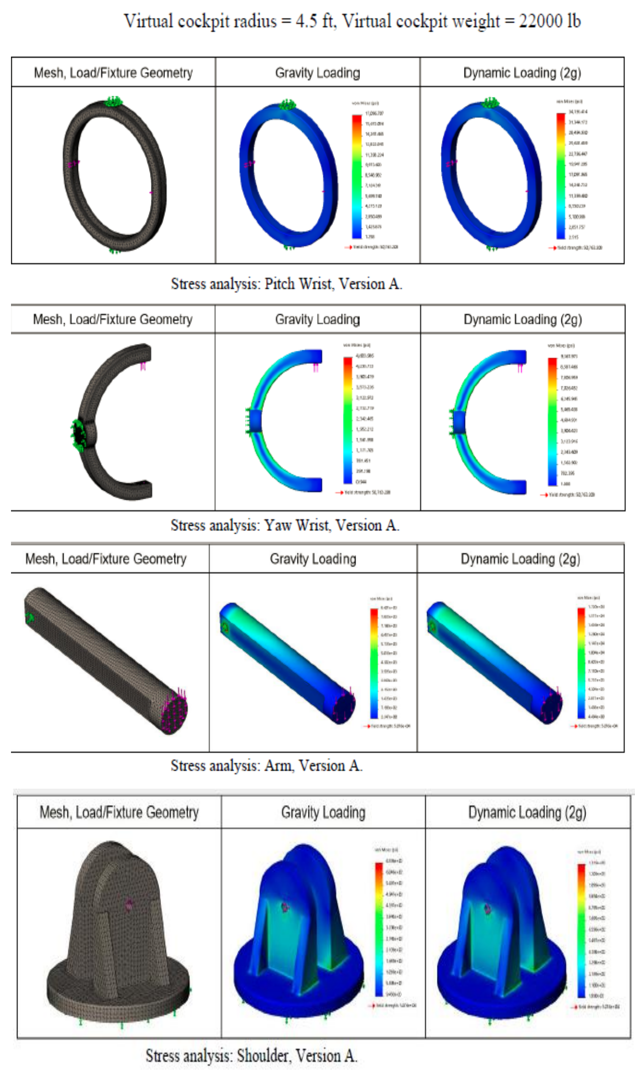

Figure 9. Stress analysis of version A

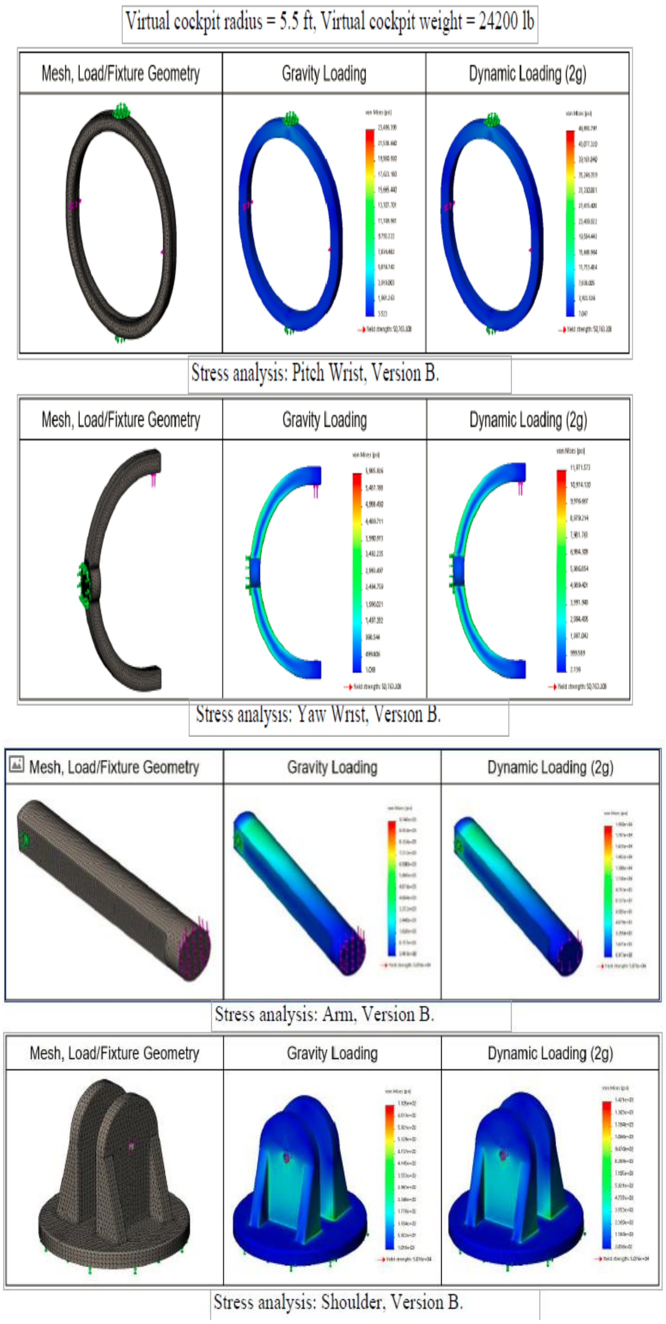

Figure 10. Stress analysis of version B

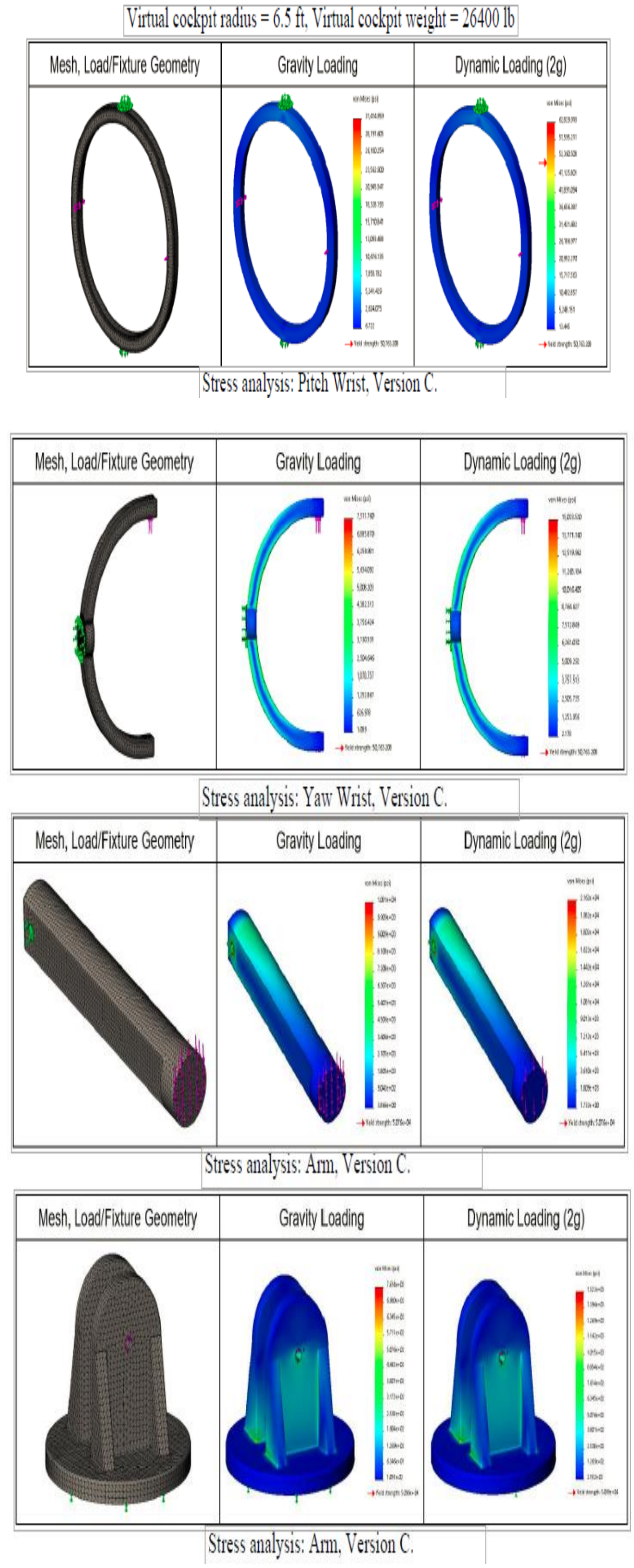

Figure 11. Stress analysis of version C

Figure 12 shows the minimum factor of safety during gravity loading for each component. The points can be observed as the maximum g-force each component can withstand. Therefore, the lowest point describes the maximum g-force each configuration can withstand. These results are tabulated in table 1 including a 1.15 factor of safety.

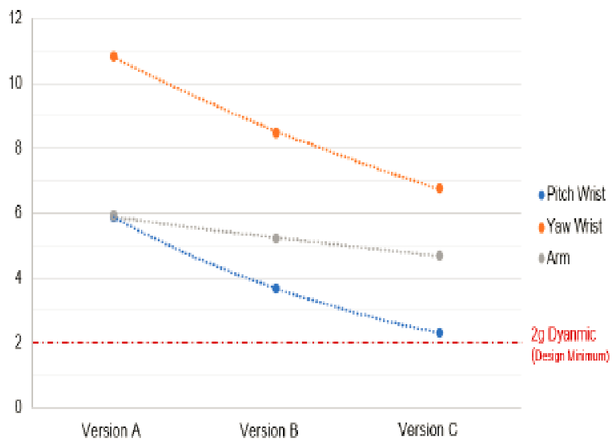

Figure 12. Gravity Loading Minimum Factor of Safety

TABLE 1. MAX SIMULATOR ACCELERATION RESULTS

Simulator Configuration	***Maximum System Acceleration***
Version A	5.11g
Version B	3.21g
Version C	2.00g

V. CONCLUSION

This design and analysis were an interesting experience in a product's design. The design of the robot arm and spherical simulator concept are atypical from conventional simulator designs but may have merit for their wide motion profile. Using the robot's main arm, pilots can experience translational motion over 2g of acceleration for each design concept. The robot's gyroscopic wrist allows the pilots to experience rotational motion in all three axes. These five axes of motion can give pilots a very accurate experience. The robotic arm succeeded in meeting the design objective of accurately simulating the motion of Boeing 747.

Designing three configurations allowed for comparison and opens opportunities for different implementations. By keeping the robots tube structure constant, the different configurations have different performance. The smallest version (A) could withstand up to 5.1g, meaning this simulator could be refitted to simulate a more aggressive motion profile, like that of a fight jet.

There are many areas for improvement in this project. To improve the accuracy of the loading conditions, motion simulation could be conducted to determine dynamic loads (as opposed to the relatively rough hand calculations). The geometry of the robot could also be furthered optimized, including the length of the robot arm, wrist geometry, and tube cross sections dimensions.

REFERENCES

[1] Meyer A. Nahon, and Lloyd D. Reid, "Simulator motion-drive algorithms - A designer's perspective", ARC, VOL., 13, 2012

[2] Lloyd D. Reid and Meyer A. Nahon, " Response of Airline Pilots to Variations in Flight Simulator Motion Algorithms", ARC, VOL., 25, 1988

[3] Eric L. Groen and Jelte E. Bos, "Simulator Sickness Depends on Frequency of the Simulator Motion Mismatch: An Observation", MIT Press, VOL 17, 2008.

[4] Nikhil J.I Garrett and Matthew C. Best, "Model predictive driving simulator motion cueing algorithm with actuator-based constraints", International Journal of Vehicle Mechanics and Mobility, VOL. 51, 2013.